Oxidative Addition of Aryl Halides to Palladium(0) Complexes: A Density-Functional Study Including Solvation

Hans Martin Senn*,† and Tom Ziegler*,‡

Department of Chemistry, University of Calgary, Calgary, Alberta T2N 1N4, Canada

Received January 13, 2004

Using density-functional theory calculations in combination with an electrostatic continuum solvation model, we have investigated the oxidative addition of phenyl halides PhX to palladium(0) complexes of bidentate phosphanes [Pd(PP)], yielding aryl halo complexes [(PP)-Pd(Ph)(X)], with X = Cl, Br, I and PP = 1,2-bis(dimethylphosphino)ethane or (*P*)-2,2′-bis-(dimethylphosphino)-1,1′-biphenyl. We have considered the formation of the reactive 14-electron species from the saturated [$Pd(PP)_2$] as well as different prereaction complexes [(PP)Pd(PhX)] with an intact phenyl halide. We find that ligand dissociation is the limiting reaction step, while the formation of the prereaction complex and the oxidative addition itself are energetically (very) favorable. The concerted transition state for oxidative addition known in the gas phase could not be found in solution. Instead, we propose a pathway involving the very facile dissociation of the halide from the prereaction complex, with subsequent collapse to the product.

Introduction

The oxidative addition of aryl halides to palladium(0) d^{10} complexes, forming palladium(II) aryl halo complexes, $[Pd^0L_m] + Ar{-}X \rightarrow [Pd^{II}L_n(Ar)(X)]$ (Ar denoting aryl throughout the paper), is a fundamental reaction in organometallic chemistry.[1,2] It constitutes an elementary step in the catalytic cycle of a series of important palladium-catalyzed reactions that transfer an aryl group onto a variety of substrates. These arylation reactions include the formation of arylamines, arylethers, and arylthioethers from amines,[3−5] alkoxides,[3,4,6] and sulfides,[3,7] respectively; of alkenyl arenes from alkenes (Heck reaction);[8] of biaryls and alkyl arenes from organoboron reagents (Suzuki coupling);[9] and of biaryls as well as alkenyl and alkynyl arenes from magnesium, aluminum, zinc, tin, or zirconium organyls (Stille, Negishi, and related cross-couplings).[10] In all these cases, the electrophilic aryl halide is oxidatively added to a palladium(0) complex before being transferred onto the other coupling partner. The Ar−X oxidative addition can even constitute the rate-limiting step of the process.

A number of experimental studies have provided insight into mechanistic aspects of the reaction, in particular with palladium(0) phosphane complexes.[11−27] Only a few of them,[22−27] however, have been concerned specifically with complexes of chelating diphosphanes, although this class of ligands is widely used. From these studies, we highlight some of the mechanistic features that have emerged: (i) Oxidative addition occurs to a coordinatively unsaturated complex. In the case of highly sterically demanding monodentate phosphanes (such as P(*o*-Tol)$_3$ or P(*t*-Bu)$_3$), even monoligated 12-electron species are involved.[16,20,28] Ligand dissociation

† Present address: Max-Planck-Institut für Kohlenforschung, D-45470 Mülheim an der Ruhr, Germany. E-mail: senn@mpi-muelheim.mpg.de.
‡ E-mail: ziegler@ucalgary.ca.

(1) Collman, J. P.; Hegedus, L. S.; Norton, J. R.; Finke, R. G. *Principles and Applications of Organotransition Metal Chemistry*; University Science: Mill Valley, CA, 1987.
(2) Stille, J. K.; Lau, K. S. Y. *Acc. Chem. Res.* **1977**, *10*, 434−442.
(3) Prim, D.; Campagne, J.-M.; Joseph, D.; Andrioletti, B. *Tetrahedron* **2002**, *58*, 2041−2075.
(4) Muci, A. R.; Buchwald, S. L. In *Cross-Coupling Reactions, A Practical Guide*; Miyaura, N., Ed.; Topics in Current Chemistry, Vol. 219; Springer: Berlin, 2002; pp 131−209.
(5) Hartwig, J. F. In *Modern Amination Methods*; Ricci, A., Ed.; Wiley-VCH: Weinheim, 2000; pp 195−262.
(6) Hartwig, J. F. *Angew. Chem., Int. Ed.* **1998**, *37*, 2046−2067.
(7) Kondo, T.; Mitsudo, T. *Chem. Rev.* **2000**, *100*, 3205−3220.
(8) Bräse, S.; de Meijere, A. In *Metal-catalyzed Cross-coupling Reactions*; Diederich, F.; Stang, P. J., Eds.; Wiley-VCH: Weinheim, 1998; pp 99−166.
(9) Suzuki, A. In *Metal-catalyzed Cross-coupling Reactions*; Diederich, F., Stang, P. J., Eds.; Wiley-VCH: Weinheim, 1998; pp 49−97.
(10) Negishi, E.-i.; Liu, F. In *Metal-catalyzed Cross-coupling Reactions*; Diederich, F., Stang, P. J., Eds.; Wiley-VCH: Weinheim, 1998; pp 1−47.
(11) Fitton, P.; Rick, E. A. *J. Organomet. Chem.* **1971**, *28*, 287−291.
(12) Fauvarques, J.-F.; Pflüger, F. *J. Organomet. Chem.* **1981**, *208*, 419−427.
(13) Amatore, C.; Pflüger, F. *Organometallics* **1990**, *9*, 2276−2232.
(14) Amatore, C.; Jutand, A.; Suarez, A. *J. Am. Chem. Soc.* **1993**, *115*, 9531−9541.
(15) Paul, F.; Patt, J.; Hartwig, J. F. *Organometallics* **1995**, *14*, 3030−3039.
(16) Hartwig, J. F.; Paul, F. *J. Am. Chem. Soc.* **1995**, *117*, 5373−5374.
(17) Casado, A. L.; Espinet, P. *Organometallics* **1998**, *17*, 954−959.
(18) Amatore, C.; Jutand, A. *Acc. Chem. Res.* **2000**, *33*, 314−321.
(19) Roy, A. H.; Hartwig, J. F. *J. Am. Chem. Soc.* **2001**, *123*, 1232−1233.
(20) Alcazar-Roman, L. M.; Hartwig, J. F. *J. Am. Chem. Soc.* **2001**, *123*, 12905−12906.
(21) Galardon, E.; Ramdeehul, S.; Brown, J. M.; Cowley, A.; Hii, K. K.; Jutand, A. *Angew. Chem., Int. Ed.* **2002**, *41*, 1760−1763.
(22) Portnoy, M.; Milstein, D. *Organometallics* **1993**, *12*, 1665−1673.
(23) Amatore, C.; Broeker, G.; Jutand, A.; Khalil, F. *J. Am. Chem. Soc.* **1997**, *119*, 5176−5185.
(24) Jutand, A.; Hii, K. K.; Thornton-Pett, M.; Brown, J. M. *Organometallics* **1999**, *18*, 5367−5374.

10.1021/om049963n CCC: $27.50
Publication on Web 05/05/2004

is therefore always a preparatory step for oxidative addition and may even be rate-delimiting.[25] (ii) For bidentate phosphanes, the only[25,26] (or at least most reactive[22]) species undergoing oxidative addition is [Pd(PP)] (PP = chelating diphosphane ligand), certainly in the absence of ligands with good π-acceptor properties, such as methyl acrylate.[24] Recently, Blackmond, Buchwald, and co-workers[27] presented evidence for the case of the Pd(BINAP)-catalyzed (BINAP = 2,2′-bis(diphenylphosphino)-1,1′-binaphthyl) amination of bromobenzene where the oxidative addition actually occurs to the amine complex [Pd(BINAP)(NHRR′)] when the amine is present in excess relative to the aryl halide. (iii) The available kinetic data[22,25,26] do not allow one to exclude the formation of a prereaction complex [(PP)Pd(ArX)], after full dissociation of the first PP ligand. Such a species, in which the Ar−X bond is still intact, is likely to be involved at high ArX concentrations.[26] (iv) The coordination of a solvent molecule directly to the reacting complex can be excluded.[25,26] (v) There is no indication (evidence for paramagnetic species, sensitivity toward radical scavengers, formation of biaryl side-products, etc.) for the participation of radical species in the reaction. A single-electron-transfer mechanism is therefore unlikely, in contrast to the situation for Ar−X oxidative addition to nickel(0) complexes.[29,30] (vi) A Hammett study using a series of substituted aryl chlorides[22] found a highly positive ρ value and a strong correlation with Hammett's σ^- constant, which suggests an S_NAr-type transition state with charge separation.

On the theoretical side, C−X oxidative addition has generally received much less attention than oxidative additions of (relatively) unpolar bonds, such as H−H, C−C, or C−H. The addition of iodomethane to square-planar rhodium(I) and iridium(I) d^8 complexes has been investigated in the context of Monsanto-type carbonylation processes.[31−33] The reactivity of three-coordinate complexes of the same metals toward activation of the C−X bond of fluoromethane[34] and the tetrahalomethanes[35] was also studied. The first study on C−X oxidative addition to a d^{10} metal center was reported by Bickelhaupt et al.,[36] who investigated the addition of chloromethane to a bare palladium atom. Comparing concerted oxidative addition, S_N2 substitution, and single-electron transfer under $Cl^•$ abstraction, they found the concerted process to be the most favorable one. Accounting for solvation (water or diethyl ether) with a simple Born−Onsager model did not change the situation qualitatively. More recently, Diefenbach and Bickelhaupt emphasized however the quantitative importance of relativistic effects for this reaction.[37] Only a few computational studies have been devoted to the oxidative addition of a C−X bond to a d^{10} complex,[38−40] all with [Pd^0L_2]. The halides and ligands involved were chloro- and bromobenzene (L = diaminocarbene);[38] iodobenzene (L_2 = 1,2-diphosphinoethane);[39] and a series of substituted alkynyl halides RC≡C−X (X = F, Cl, Br, I) and substituted fluorobenzenes (L = PH_3).[40] For iodobenzene,[39] a concerted transition state (**I**, Scheme 1) was found, in which the plane of the three reacting atoms {Pd, C_{ipso}, I} is almost perpendicular to the {P, Pd, P} coordination plane; the barrier relative to the free reactants was −16 kJ mol^{-1} (+16 kJ mol^{-1} relative to the η^2-arene prereaction complex). In the case of fluorobenzene,[40] the reaction was also concerted, but the reacting atoms lay in the coordination plane, and the barrier relative to the free reactants was 172 kJ mol^{-1}; no prereaction complex could be located. Taking solvation (water) into account using the COSMO continuum solvation model lowered the barrier by a few kJ mol^{-1}. With *ortho*-nitro-substituted fluorobenzenes, however, only the zwitterionic intermediate **II** was found in solution, rather than a concerted transition state.[40] **II** resembles the Meisenheimer intermediate of S_NAr reactions, featuring a pyramidalized C_{ipso} atom. Its elongated C−F bond suggests facile fluoride elimination, followed by collapse to the product.

Scheme 1

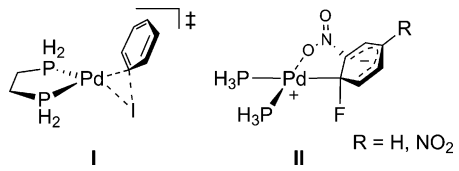

I II

In the present contribution, we have used density-functional theory calculations to investigate the oxidative addition of chloro-, bromo-, and iodobenzene to complexes of palladium with the bidentate phosphane ligands 1,2-bis(dimethylphosphino)ethane (dmpe) and (*P*)-2,2′-bis(dimethylphosphino)-1,1′-biphenyl (bimep); see Scheme 2. We focus on the nature of the transition state, contrasting a concerted with an S_NAr-type process. In particular, we consider the influence of the moderately polar solvent tetrahydrofuran (THF) on the mechanism, using the electrostatic continuum solvation model COSMO. As illustrated in ref 40, alternative pathways can become available in solution that are not viable in the gas phase; for instance, a charge-separated species such as **II** is most unlikely to be competitive in the gas phase. We also examine the formation of the reactive 14-electron complexes **2** from the tetracoordinate **1** as well as different prereaction complexes **3** with an intact phenyl halide.

(25) Alcazar-Roman, L. M.; Hartwig, J. F.; Rheingold, A. L.; Liable-Sands, L. M.; Guzei, I. A. *J. Am. Chem. Soc.* **2000**, *122*, 4618−4630.
(26) Alcazar-Roman, L. M.; Hartwig, J. F. *Organometallics* **2002**, *21*, 491−502.
(27) Singh, U. K.; Strieter, E. R.; Blackmond, D. G.; Buchwald, S. L. *J. Am. Chem. Soc.* **2002**, *124*, 14104−14114.
(28) Stambuli, J. P.; Bühl, M.; Hartwig, J. F. *J. Am. Chem. Soc.* **2002**, *124*, 9346−9347.
(29) Fahey, D. R.; Mahan, J. E. *J. Am. Chem. Soc.* **1977**, *99*, 2501−2508.
(30) Tsou, T. T.; Kochi, J. K. *J. Am. Chem. Soc.* **1979**, *101*, 6319−6332.
(31) Griffin, T. R.; Cook, D. B.; Haynes, A.; Pearson, J. M.; Monti, D.; Morris, G. E. *J. Am. Chem. Soc.* **1996**, *118*, 3029−3030.
(32) Ivanova, E. A.; Gisdakis, P.; Nasluzov, V. A.; Rubailo, A. I.; Rösch, N. *Organometallics* **2001**, *20*, 1161−1174.
(33) Cavallo, L.; Solà, M. *J. Am. Chem. Soc.* **2001**, *123*, 12294−12302.
(34) Su, M.-D.; Chu, S.-Y. *J. Am. Chem. Soc.* **1997**, *119*, 10178−10185.
(35) Su, M.-D.; Chu, S.-Y. *J. Am. Chem. Soc.* **1999**, *121*, 1045−1058.
(36) Bickelhaupt, F. M.; Ziegler, T.; Schleyer, P. v. R. *Organometallics* **1995**, *14*, 2288−2296.
(37) Diefenbach, A.; Bickelhaupt, F. M. *J. Chem. Phys.* **2001**, *115*, 4030−4040.
(38) Albert, K.; Gisdakis, P.; Rösch, N. *Organometallics* **1998**, *17*, 1608−1616.
(39) Sundermann, A.; Martin, J. M. L. *Chem. Eur. J.* **2001**, *7*, 1703−1711.
(40) Jakt, M.; Johanissen, L.; Rzepa, H. S.; Widdowson, D. A.; Wilhelm, R. *J. Chem. Soc., Perkin Trans. 2* **2002**, 576−581.

Scheme 2. Overview of Reactions Considered and Numbering Scheme

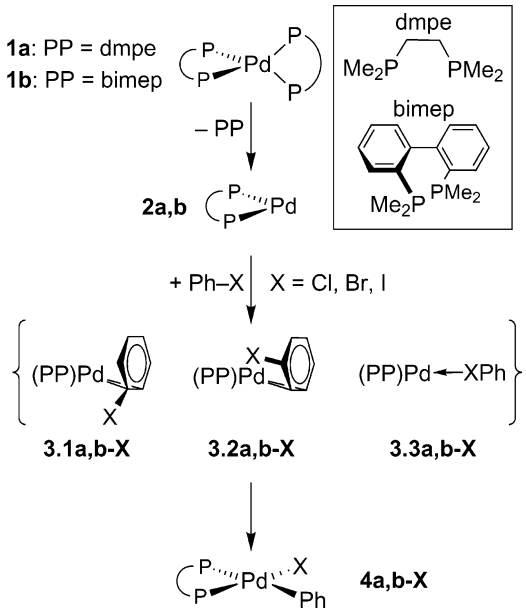

Computational Details

A. General Procedures. The calculations reported in this paper were performed with the Amsterdam Density Functional program,[41,42] release ADF 2000.02.[43] The wave functions were expanded into a basis set of Slater-type orbitals. A double-ζ basis with one polarization function (basis III) was used for H, C, and P; triple-ζ (basis IV) for Pd and I; and triple-ζ with two polarization functions (basis V) for Cl and Br. Electrons in inner shells were treated within the frozen-core approximation; the number of valence electrons retained was 1 (H), 4 (C), 5 (P), 7 (Cl, Br, I), and 18 (Pd). Scalar relativistic effects were incorporated at the level of the quasi-relativistic Pauli Hamiltonian.[44−46] The gradient-corrected exchange−correlation functional due to Becke[47] (exchange) and Perdew[48,49] (correlation) was used, with the parametrization of the correlation in the homogeneous electron gas due to Vosko, Wilk, and Nusair.[50] Both relativistic effects and gradient corrections were treated fully variationally. Structures were converged to 10^{-4} E_h (energy) and 10^{-3} E_h/Å (gradients), without any symmetry constraints. The general accuracy parameter for the numerical integration was set to 4.5, except for transition-state searches (5.5) and frequency calculations (6.0). Transition states were located manually using constrained optimizations or with a transition-state search algorithm.[51,52] Selected transition states were characterized by calculating second derivatives, using the finite-differences technique,[53,54] and by following the intrinsic reaction path[55−58] (see Supporting Information for additional details).

B. Solvation Effects. The solvent was described as a homogeneous, isotropic, linear dielectric medium within the conductor-like screening model (COSMO) due to Klamt and Schüürmann[59,60] as implemented in ADF.[61] The cavity containing the solute molecule was bounded by a solvent-excluding surface constructed with a solvent radius of 1.4 Å and parameters ndiv = 4, min = 0.5, and ofac = 0.8. The scaling factor correcting the conductor results for finite dielectric behavior was $f = (\epsilon_r - 1)/\epsilon_r$; the dielectric constant for THF is $\epsilon_r = 7.52$ at 295 K.[62] Nonelectrostatic contributions to solvation were not considered. The solvation effects were included self-consistently in the calculations, and structures were optimized including solvation. The calculated solvation energies were obtained as $\Delta_{solv}G = G^{sol} - E^g$, where G^{sol} is the energy in solution (electronic energy including solvation contributions), and E^g is the electronic energy in the gas phase.

For the determination of the solvation radii, it was recognized that the single most important contribution to solvation in the systems of interest stems from the dissociated halide ion. The solvation radii for the halogens were therefore adjusted to reproduce the experimental solvation free energy of the respective halide in THF, $\Delta_{solv}G(X^-; THF)$, X = Cl, Br, I. Such data are, unfortunately, very scarce. We were able to obtain $\Delta_{solv}G(X^-; THF)$ by combining hydration free energies, $\Delta_{solv}G(X^-; H_2O)$, with free energies of transfer, $\Delta_tG(X^-; H_2O \rightarrow THF)$. For the hydration free energy of X^-, the average of the values given in refs 63 and 64 was used. Note that the former values refer to a standard state in the gas phase of 1 bar and were converted to refer to 1 mol L^{-1}; all these hydration energies rest on the absolute value for the proton as reevaluated by Tissandier et al.[65] The free energies for the transfer of X^- from H_2O to THF were taken from ref 66. The $\Delta_{solv}G(X^-; THF)$ values thus obtained are −267, −237, and −196 kJ mol^{-1} for Cl, Br, and I, respectively. The solvation radii derived from these are 2.1, 2.4, and 3.0 Å for Cl, Br, I; the radii used for H and C are 1.16 and 2.0 Å, respectively.[67] This set of radii was validated by comparing calculated to experimental (from the Supporting Information of ref 68) solvation free energies of PhR (R = H, Me, Cl, Br) and *p*-dichlorobenzene in THF, Et_2O, and CH_2Cl_2. They were found to agree within 3 kJ mol^{-1}, except for *p*-dichlorobenzene in Et_2O, where the deviation was 8 kJ mol^{-1}. Due to the lack of experimental data, the radii for P and Pd were set to 120% of the respective van der Waals radius,[69] i.e., at 2.2 (P) and 1.92 Å (Pd). It was verified that these latter radii have only a negligible influence on the solvation energy of compounds

(41) te Velde, G.; Bickelhaupt, F. M.; Baerends, E. J.; Fonseca Guerra, C.; van Gisbergen, S. J. A.; Snijders, J. G.; Ziegler, T. *J. Comput. Chem.* **2001**, *22*, 931−967.
(42) Fonseca Guerra, C.; Snijders, J. G.; te Velde, G.; Baerends, E. J. *Theor. Chem. Acc.* **1998**, *99*, 391−403.
(43) *ADF*, release 2000.02; SCM, Theoretical Chemistry, Vrije Universiteit: Amsterdam, The Netherlands; http://www.scm.com/.
(44) Snijders, J. G.; Baerends, E. J.; Ros, P. *Mol. Phys.* **1979**, *38*, 1909−1929.
(45) Boerrigter, P. M.; Baerends, E. J.; Snijders, J. G. *Chem. Phys.* **1988**, *122*, 357−374.
(46) Ziegler, T.; Tschinke, V.; Baerends, E. J.; Sijders, J. G.; Ravenek, W. *J. Phys. Chem.* **1989**, *93*, 3050−3056.
(47) Becke, A. D. *Phys. Rev. A* **1988**, *38*, 3098−3100.
(48) Perdew, J. P. *Phys. Rev. B* **1986**, *33*, 8822−8824.
(49) Perdew, J. P. *Phys. Rev. B* **1986**, *34*, 7406.
(50) Vosko, S. H.; Wilk, L.; Nusair, M. *Can. J. Phys.* **1980**, *58*, 1200−1211.
(51) Versluis, L.; Ziegler, T. *J. Chem. Phys.* **1988**, *88*, 322−328.
(52) Fan, L.; Ziegler, T. *J. Am. Chem. Soc.* **1991**, *114*, 10890−10897.
(53) Fan, L.; Ziegler, T. *J. Chem. Phys.* **1992**, *96*, 9005−9012.
(54) Fan, L.; Ziegler, T. *J. Phys. Chem.* **1992**, *96*, 6937−6941.
(55) Fukui, K. *J. Phys. Chem.* **1970**, *74*, 4161−4163.
(56) Fukui, K. *Acc. Chem. Res.* **1981**, *14*, 363−368.
(57) Deng, L.; Ziegler, T.; Fan, L. *J. Chem. Phys.* **1993**, *99*, 3823−3835.
(58) Deng, L.; Ziegler, T. *Int. J. Quantum Chem.* **1994**, *52*, 731−765.
(59) Klamt, A.; Schüürmann, G. *J. Chem. Soc., Perkin Trans. 2* **1993**, 799−805.
(60) Klamt, A. In *Encyclopedia of Computational Chemistry*; Schleyer, P. v. R., Ed.; Wiley: Chichester, 1998; Vol. 1, pp 604−615.
(61) Pye, C. C.; Ziegler, T. *Theor. Chem. Acc.* **1999**, *101*, 396−408.
(62) Lide, D. R., Ed. *CRC Handbook of Chemistry and Physics*, 3rd electronic ed.; http://www.knovel.com/, 2000.
(63) Fawcett, W. R. *J. Phys. Chem. B* **1999**, *103*, 11181−11185.
(64) Pliego, J. R., Jr.; Riveros, J. M. *Chem. Phys. Lett.* **2000**, *332*, 597−602.
(65) Tissandier, M. D.; Cowen, K. A.; Feng, W. Y.; Gundlach, E.; Cohen, M. H.; Earhart, A. D.; Coe, J. V.; Tuttle, T. R., Jr. *J. Phys. Chem. A* **1998**, *102*, 7787−7794.
(66) Elsemongy, M. M.; Abdel-Khalek, A. A. *Thermochim. Acta* **1991**, *181*, 79−94.
(67) Chan, M. S. W.; Vanka, K.; Pye, C. C.; Ziegler, T. *Organometallics* **1999**, *18*, 4624−4636.
(68) Hawkins, G. D.; Liotard, D. A.; Cramer, C. J.; Truhlar, D. G. *J. Org. Chem.* **1998**, *63*, 4305−4313.
(69) Bondi, A. *J. Phys. Chem.* **1964**, *68*, 441−451.

Table 1. Reaction Energies in the Gas Phase and in THF Solution for Ligand Dissociation (1 → 2 + PP), Formation of Prereaction Complexes (2 + PhX → 3), Oxidative Addition (3.1 → 4), and Halide Dissociation (3.1 → $4^+ + X^-$)

		$\Delta_r E$/(kJ mol^{-1})			
		dmpe (**a**)		bimep (**b**)	
step	X	g	THF	g	THF
1 → 2		189	175	169	145
2 → 3.1-X	Cl	−74	−78	−57	−55
	Br	−82	−88	−65	−63
	I	−94	−100	−76	−75
2 → 3.2-X	Cl	−87	−85	−70	−62
	Br	−88	−85	−71	−62
	I	−89	−85	−71	−62
2 → 3.3-X	Cl	−20	−20	−21	−16
	Br	−33	−37	−32	−27
	I	−44	−48	−37	−33
3.1-X → 4-X	Cl	−99	−142	−90	−123
	Br	−121	−155	−111	−136
	I	−130	−156	−117	−136
3.1-X → 4^+	Cl		4		19
	Br		−12		2
	I		−10		3

containing these atoms. This is due to the fact that these atoms are typically surrounded by at least three substituents or ligands, such that they do not appreciably contribute to the molecular surface. For instance, the solvation energy of PPh_3 does not change within 1 kJ mol^{-1} when varying the P solvation radius between 2.0 and 2.75 Å.

Results and Discussion

A. Ligand Dissociation. In the first step, we considered the formation of the coordinatively unsaturated 14-electron species [Pd(PP)] (**2a** with PP = dmpe; **2b** with PP = bimep) from the corresponding saturated [Pd(PP)$_2$] (**1a**, **b)** by dissociation of one of the bidentate ligands. This process is energetically disfavored by 145−190 kJ mol^{-1} (see Table 1 and Figure 1), with dmpe requiring ∼25 kJ mol^{-1} more in energy than bimep. Upon solvation, the positive reaction energies are lowered by ∼20 kJ mol^{-1} owing to the gain in solvation energy stemming from the free ligand (see solvation energies in Table 2). Structurally, we found the expected changes in the geometry of the complex when decreasing the coordination number. Compared to the tetrahedral **1**, the two remaining Pd−P bonds in **2** shorten to compensate for the lost metal−ligand bonding and the P−Pd angle opens up (see structures in Figure 2). The increase in the bite angle, which brings the coordination geometry closer to the linear arrangement electronically preferred in ML_2 d^{10} complexes,[70] is larger for bimep than for dmpe. The seven-membered chelate ring of the former can accommodate a larger bite angle than the five-membered ring of the latter, which also accounts for the less unfavorable dissociation energy for bimep. There is essentially no influence of solvation on the structures of **1** and **2**.

B. Prereaction Complexes. Aryl halides, which can act as electron-accepting ligands, could form stable complexes with the electron-rich, unsaturated [Pd(PP)] fragment and were thus investigated as potential prereaction complexes in Ar−X activation. There are in principle several coordination modes conceivable for an aryl halide. In analogy with the related oxidative addition of aryl C−H bonds, where, for example, platinum(0),[71] platinum(II),[72] or rhodium(I)[73] η^2-arene complexes were experimentally shown to be involved, we considered the coordination of the aryl halide in an η^2 fashion. Both [(PP)Pd{(1,2η)-PhX}] (**3.1-X**) and [(PP)Pd{(2,3η)-PhX}] (**3.2-X**) complexes were studied, in which, respectively, the $C_{ipso}-C_{ortho}$ or the $C_{ortho}-C_{meta}$ bond of the aryl halide coordinates to the metal center. Another possibility is the monodentate coordination through the halogen atom, as demonstrated for a group 10 metal in $[\{P(i\text{-}Pr)_3\}_2Pt(H)(PhX\text{-}\kappa X)]^+$ (X = Br, I).[74] We therefore also considered the complexes [(PP)Pd(PhX-κX)] (**3.3-X**).

Reaction energies for the coordination of Ph−X (X = Cl, Br, I) to **2**, yielding **3.1**−**3.3**, are collected in Table 1, and optimized structures are shown in Figure 3. The reaction is exothermic in all cases, irrespective of the combination of ligand, phenyl halide, and solvation state. The η^2-arene complexes **3.1** and **3.2** are generally favored over **3.3**, the electron-accepting arene being a better suited ligand for the electron-rich d^{10} metal center. The dmpe complexes **3.1a** and **3.2a** are more stable than their bimep analogues **3.1b** and **3.2b** by ∼20 kJ mol^{-1}. This preference for dmpe in the formation of the prereaction complexes almost fully compensates the advantage of bimep in the preceding dissociation step, making the dmpe and bimep arene complexes equally stable relative to **1** (cf. Figure 1). The influence of solvation on the energetics of the formation of the prereaction complexes **3.1**−**3.3** is generally small, varying between −6 and +9 kJ mol^{-1}. A notable difference between the (1,2η)-arene complexes **3.1** and the (2,3η) complexes **3.2** is the influence of the halide. Whereas the formation of **3.1**, where the aryl halide C_{ipso} atom is directly attached to the palladium, becomes more favorable along the series Cl < Br < I, the stability of **3.2**, where C_{ipso} is one position away from the ring atoms interacting with the metal, remains unaffected by the halide.

The structures of the Pd(PP) moiety in **3.1**−**3.3** (Figure 3) reflect the strength of the interaction with the aryl halide ligand. In the arene complexes **3.1** and **3.2**, the Pd−P bond lengths and the P−Pd−P angle take values similar to those in the coordinatively saturated **1**. In **3.3** on the other hand, where the aryl halide is relatively weakly coordinated, the Pd(PP) fragment is structurally closer to the unsaturated **2** with shorter Pd−P bonds and a wider bite angle. These differences are only weakly affected by the type of diphosphane ligand or halide; solvation slightly (∼0.02 Å) elongates the Pd−P bonds. The η^2 coordination of the arene ring to the metal in **3.1** and **3.2** is unsymmetric. The carbon atom closer to the halide (that is, C_{ipso} in **3.1** and C_{ortho} in **3.2**) is always more strongly coordinated than the other carbon. This difference Δ between the two Pd−C bond lengths varies significantly for the different arene complexes. In **3.1a** in the gas phase, it increases along

(70) Albright, T. A.; Burdett, J. K.; Whangbo, M.-H. *Orbital Interactions in Chemistry*; Wiley: New York, 1985.

(71) Iverson, C. N.; Lachicotte, R. J.; Müller, C.; Jones, W. D. *Organometallics* **2002**, *21*, 5320−5333.

(72) Reinartz, S.; White, P. S.; Brookhart, M.; Templeton, J. L. *J. Am. Chem. Soc.* **2001**, *123*, 12724−12725.

(73) Jones, W. D.; Feher, F. J. *J. Am. Chem. Soc.* **1984**, *106*, 1650−1663.

(74) Butts, M. D.; Scott, B. L.; Kubas, G. J. *J. Am. Chem. Soc.* **1996**, *118*, 11831−11843.

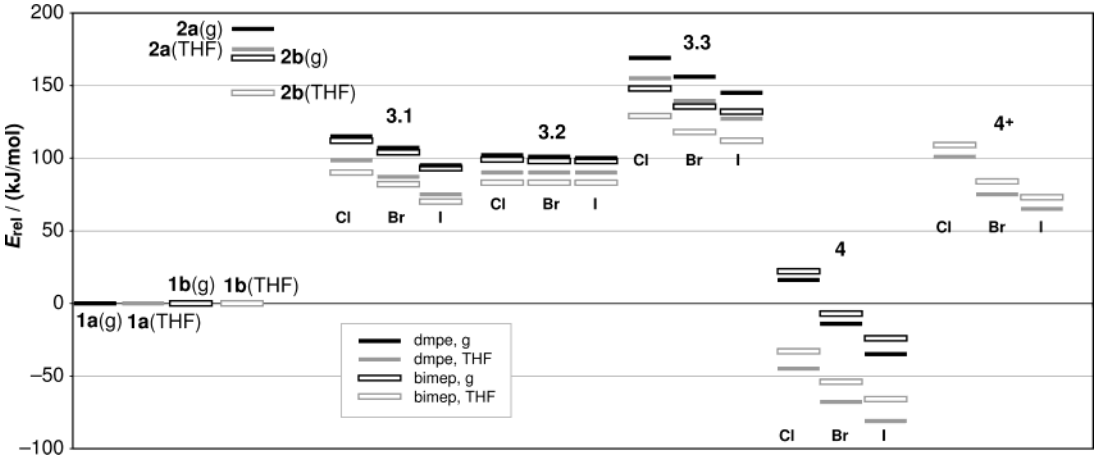

Figure 1. Relative energies of optimized complexes. The energies of all complexes **1** (with either dmpe or bimep, either in the gas phase or in THF) have been set to zero as reference point of the scale.

Table 2. Solvation Energies in THF

	$\Delta_{solv}G$/(kJ mol^{-1})
dmpe (**a**)	−27
bimep (**b**)	−47

	dmpe (**a**)	bimep (**b**)
1	−40	−68
2	−27	−45

	Cl	Br	I
X^-	−267	−238	−195
Ph−X	−22	−22	−22

	dmpe (**a**)			bimep (**b**)		
	Cl	Br	I	Cl	Br	I
3.1-X	−53	−55	−56	−65	−66	−66
3.2-X	−47	−46	−45	−59	−59	−59
3.3-X	−49	−52	−53	−62	−63	−64
4-X	−96	−89	−81	−98	−91	−85

the series Cl < Br < I from 0.04 to 0.13 Å; in THF solution, it is another ∼0.03 Å larger. In **3.2a**, however, Δ ≃ 0.02 Å irrespective of the halide or the solvation state. The same pattern is observed for the corresponding bimep complexes **3.1b** and **3.2b**, although slightly less pronounced. The strength of the Pd−C interaction is mirrored in the C−X bond: the shorter/stronger is Pd−C, the longer/weaker is C−X. Hence, in **3.1a** in the gas phase, C−X is elongated by 0.06 (X = Cl) to 0.12 Å (X = I) relative to the free aryl halide. An additional elongation of 0.03 Å (Cl) to 0.08 Å (I) is found in solution. For **3.2a**, the lengthening is small (0.02 Å) and independent of halide and solvation state. Again, the structural effects are analogous but smaller in **3.1b** and **3.2b**. The length of the C−X bond in the PhX-κX complexes **3.3** shows a dependence on halide and solvation similar to that in **3.1**. The elongation increases from 0.05 (Cl) to 0.13 Å (I) in **3.3a**(g); it is larger in solution and less marked in **3.3b**. Finally, the arene C−C bond coordinated to the metal in **3.1** and **3.2** is in all cases 0.05 Å longer than in the free aryl halide.

The trend observed in **3.1** of increasing Ph−X bond activation and better stabilization along the series Cl < Br < I can be rationalized by inspection of the pertinent orbitals involved in the interaction between the phenyl halide and the metal complex (Figure 4). The interaction is dominated by back-bonding from the electron-rich palladium(0) d^{10} center of **2** to the phenyl halide acting as the acceptor. All three phenyl halides have two low-lying empty orbitals of $C_{ipso}-C_{ortho}$ and $C_{ortho}-C_{meta}$ π-antibonding character, respectively, suitable to interact with a filled d orbital of palladium, which accounts for the η^2 coordination mode in both **3.1** and **3.2**. The energies of these orbitals are essentially unaffected by the halide. However, there is a low-lying σ^*_{C-X}-antibonding orbital that is the more strongly stabilized the less electronegative X is. Its energy decreases from −0.76 eV in PhCl to −2.25 eV in PhI, where it even becomes the lowest-lying molecular orbital (LUMO), while it is LUMO + 2 in PhCl and PhBr. This orbital can participate in metal−PhX bonding only in **3.1**, not in **3.2**, and hence this explains the halide dependence of stability and C−X bond activation in **3.1**. It also accounts for the trends observed in **3.3**.

Summarizing the results for the prereaction complexes **3.1** to **3.3**, we note that all three types are stable relative to the unsaturated complex **2** for all combinations of diphosphane, halide, and solvation state considered. The C−X bond is in all cases activated to some extent. The PhX-κX complexes **3.3** are the least favored. Moreover, in the context of Ar−X oxidative addition, they appear to be of potential interest only as intermediates in an inner-shell single-electron-transfer mechanism (leading to a Pd(I) species and an aryl radical). Such a mechanism is, however, experimentally not supported, and we will thus not consider complexes **3.3** further. The η^2-arene complexes **3.1** and **3.2** are of comparable stability. However, the C−X bond is more strongly activated in **3.1** due to the more favorable interaction of the metal complex with the phenyl halide. Furthermore, in **3.1** the Ph−X bond is suitably oriented relative to the metal center for a concerted oxidative addition process. Therefore, we focus in the following on **3.1** as prereaction complexes.

C. Oxidative Addition. 1. Phenyl Halo Complexes. The product of oxidative addition of PhX to **2** are the palladium(II) phenyl halo complexes **4** (Figure 5).Their formation (relative to the prereaction complexes **3.1**) is very energetically favored, with reaction energies in the gas phase ranging between −90 and −130 kJ mol^{-1} (see Table 1 and Figure 1). The exothermicity increases along the series Cl < Br < I. The ligand influence is small, the reaction being some 10 kJ mol^{-1}

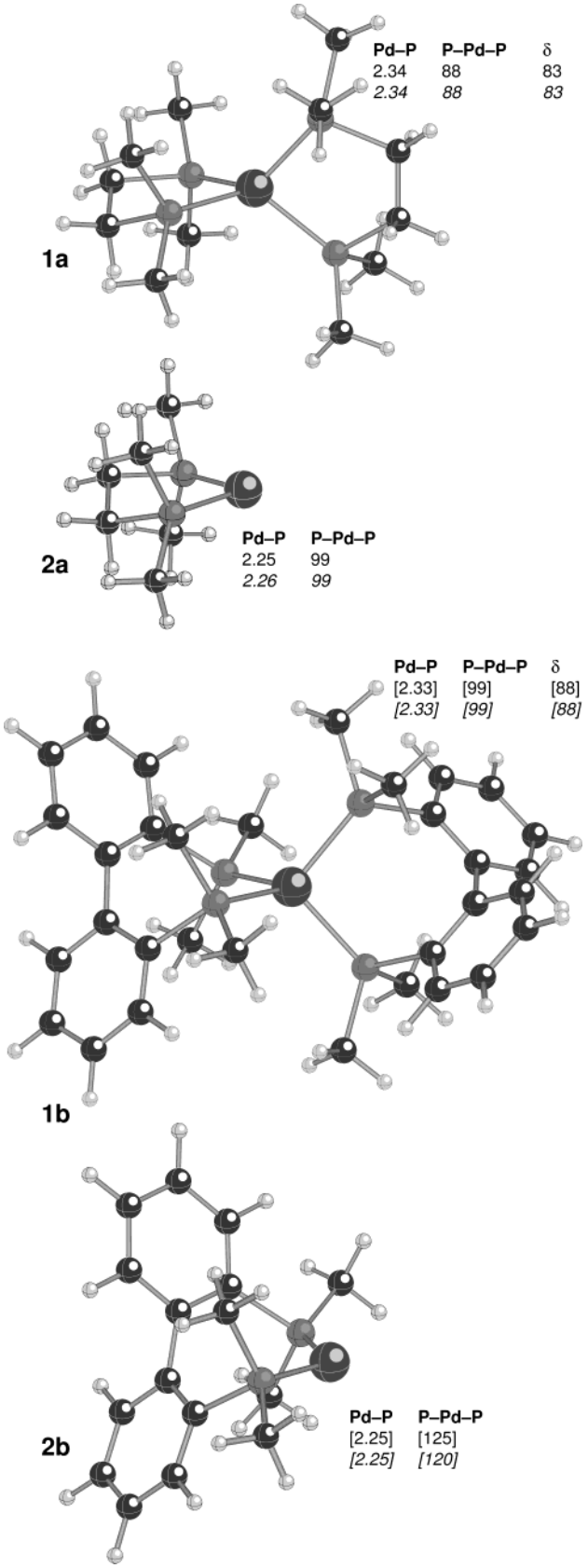

Figure 2. Optimized structures of complexes **1** and **2**. Selected bond lengths (in Å) and angles (in deg) are given. Roman type: gas phase; italics: THF solution; brackets: bimep complexes. Average values for Pd−P and P−Pd−P are given if the variation is less than 0.01 Å or 1°, respectively. δ designates the angle between the two {P, Pd, P} planes in **1**.

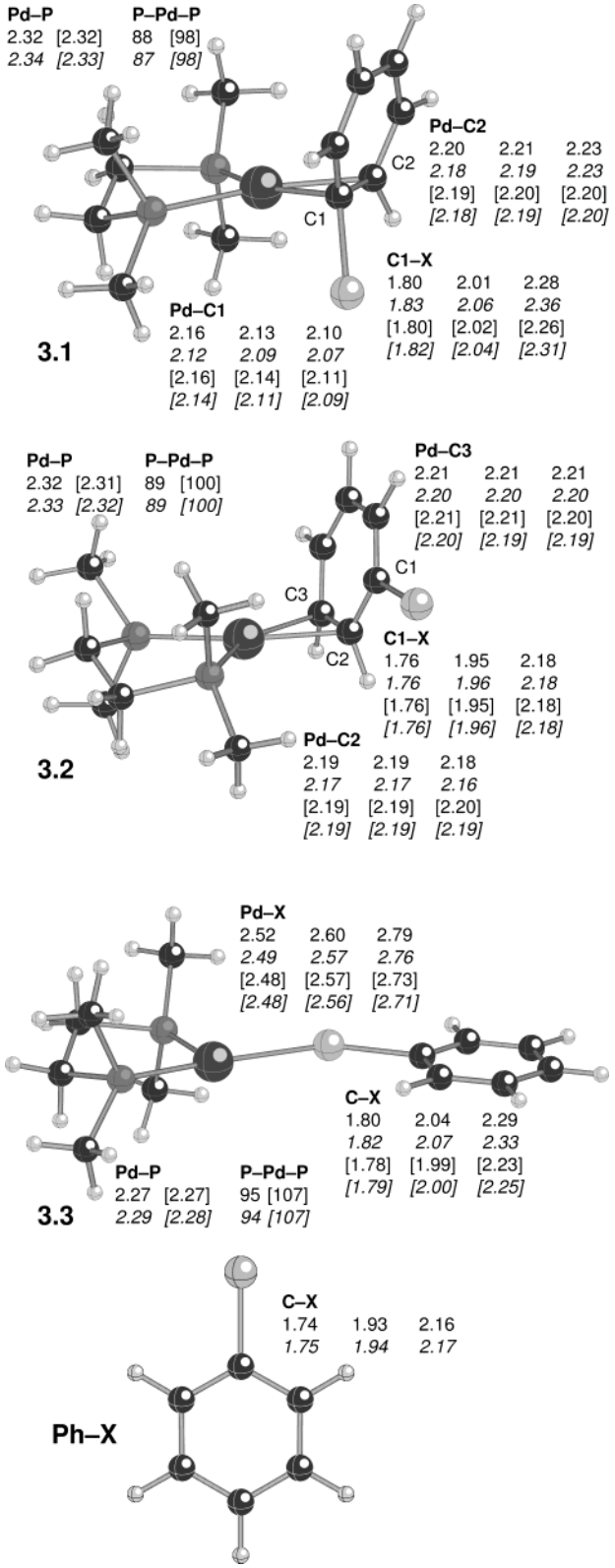

Figure 3. Optimized structures of the prereaction complexes **3.1**−**3.3**. Where structural data are arranged in three columns, they refer to the chloro, bromo, and iodo compound, respectively; see caption to Figure 2 for further explanations.

more favorable with dmpe than with bimep. Solvation, however, is important since it makes the reaction more exothermic by several tens of kJ mol^{-1}. The good solvation of complexes **4**, which have the highest solvation energies of all neutral species considered in this

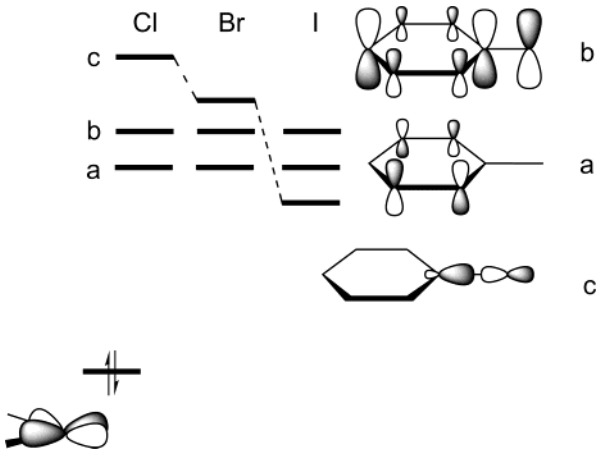

Figure 4. Sketch of the orbitals involved in the interaction between the [Pd(PP)] complex **2** and the phenyl halide. Depicted are the HOMO of **2** and the three lowest unoccupied levels of PhX. The orbital (c) is significantly stabilized along the series Cl < Br < I.

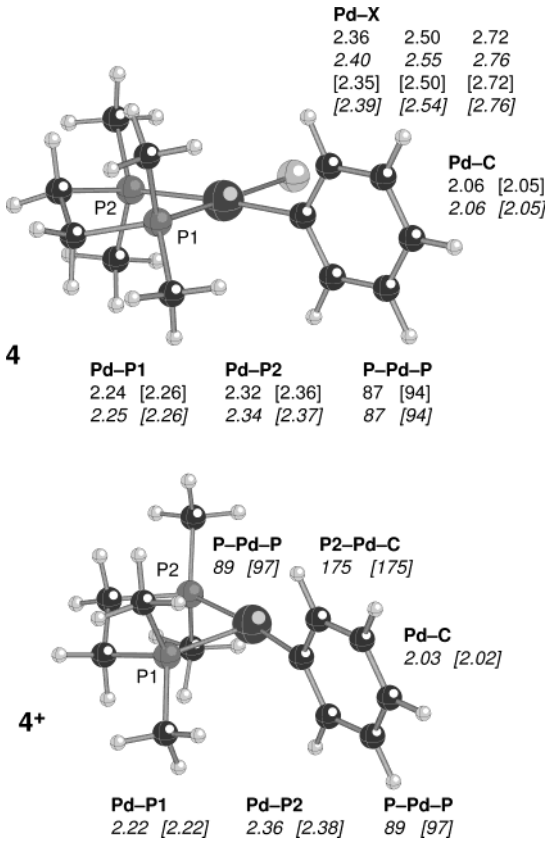

Figure 5. Optimized structures of the aryl halo complexes **4** and cationic aryl complexes $\mathbf{4}^+$. See captions to Figures 2 and 3 for explanations.

study (see Table 2), is mainly due to the accretion of charge on the electronegative halide ligand, which is well-exposed to the solvent. In the gas phase [**4a**(g)], the halide bears a Hirshfeld charge[75] of $-0.37e$ to $-0.31e$, decreasing in absolute value with electronegativity from Cl to I, concomitantly with the solvation energy. The solvation process reinforces this charge accumulation, resulting in an additional $-0.1e$ on the halide. Whereas the product complexes **4a** and **4b** are equally well solvated, the reactant **3.1b** is better solvated than **3.1a**, which reduces the favorable solvation effect by 10 kJ mol^{-1} for the reaction with the bimep complexes.

The structures of the phenyl halo complexes **4** are unobtrusive. Their coordination geometry is almost perfectly square-planar, as expected for a d^8 complex, with angles around the palladium close to 90°. The Pd−P bond trans to phenyl is ∼0.1 Å longer than the bond trans to the halide due to the strong trans influence of the phenyl ligand. The Pd−X bond is lengthened in solution by 0.04 Å, reflecting the stronger polarization. These features are independent of the halide and the phosphane ligand.

2. Transition States. In the gas phase, the existence of a concerted transition state for Ar−X oxidative addition to ML_2 d^{10} metal centers is well-established.[39,40] This transition state is characterized by a three-center interaction involving C_{ipso}, X, and M (see **I** in Scheme 1) and the concomitant breaking of the C−X bond and formation of M−C and M−X bonds. The degree of charge separation at the transition state appears to be rather moderate.[39] An interesting observation, for which a conclusive explanation remains to be presented, is that the plane defined by the three reacting atoms {M, C_{ipso}, X} is perpendicular to the coordination plane {L, M, L} for X = I,[39] but parallel for X = F.[40] For the related oxidative addition reactions of C−H, Si−H, C−C, C−Si, C−Ge, and C−Sn bonds to ML_2 d^{10} complexes, the influence of various factors (atom type and substitution pattern of the activated bond, type and nature of ligands, metal) on the transition-state structure was recently explored.[76−80]

Here, however, we focus on the transition state in solution. We located the transition state **TS1** (Figure 6) starting from **3.1a**, which structurally looks like a transition state of type **I** for a concerted oxidative addition. The activation barrier to reach **TS1** from **3.1a-X** is 39 and 11 kJ mol^{-1} for X = Cl and Br, respectively. However, following the intrinsic reaction path down from **TS1** revealed that this stationary point does not connect **3.1a** with **4**, but in fact belongs to a ring-rotation process converting the (1,2η)-arene complex into the (1,6η)-arene complex. Despite an extensive and careful search, we were unable to locate a transition state belonging to a concerted oxidative addition in solution.

As an alternative conceivable only in solution, we then studied the possibility of a dissociative process, that is, dissociation of the halide, followed by collapse to the product. The corresponding transition states **TS2** for the dissociation of the halide could indeed be located and were confirmed by frequency and IRC calculations. They feature a very elongated C−X bond and a fully developed Pd−C single bond (see Figure 6). The barrier from **3.1a-X**(THF) is low; $\Delta E^{\ddagger} = 31$, 12, and 5 kJ mol^{-1} for X = Cl, Br, and I, respectively. For the full dissociation of the halide, yielding separated X^-(THF) and the cationic

(75) Hirshfeld, F. L. *Theor. Chim. Acta* **1977**, *44*, 129.

(76) Sakaki, S.; Mizoe, N.; Musashi, Y.; Biswas, B.; Sugimoto, M. *J. Phys. Chem. A* **1998**, *102*, 8027−8036.
(77) Matsubara, T.; Hirao, K. *Organometallics* **2002**, *21*, 2662−2673.
(78) Matsubara, T.; Hirao, K. *Organometallics* **2002**, *21*, 4482−4489.
(79) Matsubara, T. *Organometallics* **2003**, *22*, 4286−4296.
(80) Giorgi, G.; De Angelis, F.; Re, N.; Sgamellotti, A. *Chem. Phys. Lett.* **2002**, *364*, 87−92.

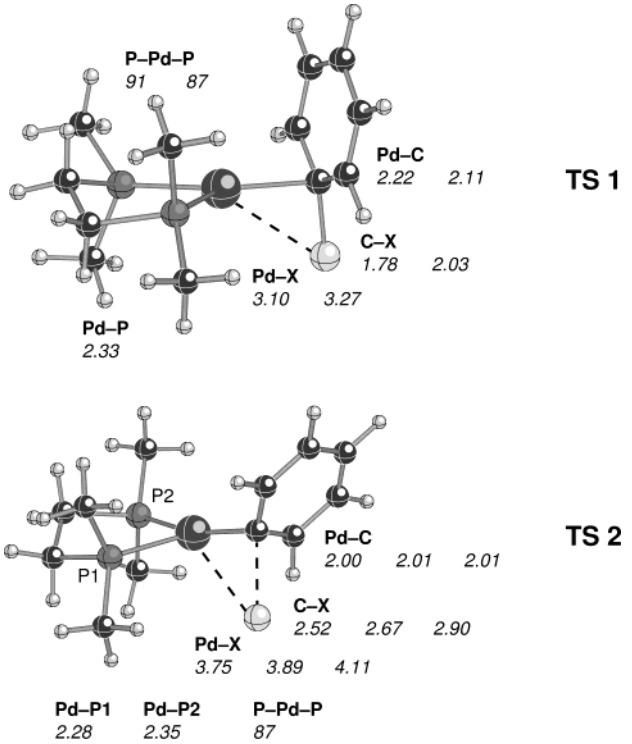

Figure 6. Optimized transition-state structures in solution. **TS1** corresponds to a rotation of the phenyl ring; **TS2**, to dissociation of the halide. See captions to Figures 2 and 3 for explanations.

phenyl complexes $\mathbf{4}^{+}$(THF), the reaction energies are essentially thermoneutral (Table 1). At the transition state, we find a significant separation of charge. The aryl halide moiety bears a Hirshfeld charge of $-0.81e$ to $-0.78e$ (slightly decreasing along Cl > Br > I), of which $-0.53e$ to $-0.48e$ are located on the halide alone. These values are to be compared to the considerably smaller charge separation in **3.1a**(THF), where the charge on the coordinated aryl halide amounts to about $-0.53e$, of which $-0.15e$ is on the halide.

Considering these findings, the following picture emerges for the oxidative addition reaction. In solution, the dissociation of the halide from the coordinated haloarene is kinetically and thermodynamically facile. Taking into account entropic contributions will make it even more favorable. Thereafter, the collapse to the aryl halo complex is an energetically strongly favored and most likely barrier-free process. This depiction remains essentially unchanged if one considers that the halide will in reality not be separated to infinity from the complex, but rather form a type of ion pair. Whereas the data obtained do not allow us to exclude rigorously the existence of a concerted transition state also in solution, they suggest that the dissociative pathway delineated here is certainly a very viable and competitive one. Corroborating experimental evidence is provided by the Hammett study indicating a charge-separated transition state.[22] The observation[40] of the Meisenheimer-type intermediate **II** (Scheme 1) for *ortho*-nitrofluorobenzene fits in as a special case where the transition state is so strongly stabilized by the electron-withdrawing substituents and coordination of the nitro group to the metal that it actually becomes an intermediate.

IV. Conclusions

We have investigated the oxidative addition of chloro-, bromo-, and iodobenzene to palladium(0) complexes bearing the bidentate chelating phosphane ligands dmpe or bimep, using density-functional theory calculations in combination with a continuum solvation model. This reaction is topical to many catalytic cycles and a fundamental reaction of organometallic chemistry. We considered first the ligand dissociation step converting the coordinatively saturated [Pd(PP)$_2$] into the reactive 14-electron species [Pd(PP)] and the formation of different prereaction complexes [(PP)Pd(PhX)] with an intact phenyl halide. The formation of [Pd(PP)] is strongly endothermic ($\Delta_r E$ = 170−190 kJ mol^{-1}, ∼20 kJ mol^{-1} less in solution), constituting the most unfavorable of the reaction steps considered here. The following association of the aryl halide is energetically favored for all combinations of coordination mode [(1,2η), (2,3η), or κX], halide, ligand, and solvation state. The aryl halides preferably bind in an η^2 fashion, acting as π-acceptor ligands stabilizing the electron-rich d^{10} center. In the (1,2η) complexes, the Ph−X bond is particularly activated. We therefore considered them as primary precursors for the oxidative addition step.

The oxidative addition itself is a strongly exothermic reaction ($\Delta_r E$ = −90 to −130 kJ mol^{-1} in the gas phase relative to the (1,2η)-arene complexes) that profits significantly from solvation, making it another 20−40 kJ mol^{-1} more favorable. The reaction is even exothermic relative to the stable, saturated [Pd(PP)$_2$] complexes (except for chlorobenzene in the gas phase). Regarding the type and structure of the transition state, the concerted transition state reported for the gas phase could not be confirmed in solution. However, we found that, owing to solvation, the dissociation of the halide is an exceedingly kinetically facile process, $\Delta E^{\ddagger}$ = 5−30 kJ mol^{-1}. Energetically, complete separation into a cationic phenyl complex and a free halide is essentially thermoneutral, not accounting for favorable entropic contributions. The subsequent recombination of the halide anion with the cationic phenyl complex is then strongly exothermic and most likely barrier-free. Considering the oxidative addition process as a whole, it is an easy reaction in the systems studied here, once the reactive 14-electron species has been generated. After ligand dissociation, which thus constitutes the limiting step, the reaction path is energetically all downhill.

We conclude with some comments on the usefulness of solvation models for mechanistic investigations. Our studies have shown that even the very basic description of solvation at the level of a continuum model is sufficient for qualitatively new insights to be gained that would not have been accessible through gas-phase calculations alone, such as the halide dissociation pathway for oxidative addition described here. However, it is essential in such work that the solvation model can be applied self-consistently in geometry optimizations. The value of a simple continuum solvation model is obviously restricted to cases where a specific interaction (e.g., coordination) of a solvent molecule to the solute is not decisive. Quantitatively, we note that the solvation contribution to reaction energies can be sizable even if only neutral species are involved, up to some 60 kJ mol^{-1} for the systems investigated here.

Acknowledgment. H.M.S. gratefully acknowledges a postdoctoral fellowship from the Swiss National Science Foundation. He thanks Dr. Sven Tobisch (Martin Luther University, Halle-Wittenberg, Germany) for stimulating discussions. This work was also supported by the donors of the Petroleum Research Fund, administered by the American Chemical Society (ACS-PRF No. 36543-AC3), and by the Natural Sciences and Engineering Research Council of Canada (NSERC). T.Z. thanks the Canadian government for a Canada Research Chair (2002).

Supporting Information Available: Cartesian coordinates of all optimized structures in Xmol xyz format (raw text) and technical details on transition-state searches (PDF). This material is available free of charge via the Internet at http://pubs.acs.org.

OM049963N